50 Years of Innovation: Cryogenics and Superconductivity in Biomedical Applications

Quan-Sheng Shu[1], Ray Radebaugh[2], Robert L. Fagaly[3]

[1]CryoSPC.com, Keller Texas 76248 USA
[2]National Institute of Standards and Technology, Boulder Colorado 80305 USA
[3]Tristan Technology (retired), Carlsbad California 92009, USA

Email: qs.shu@cryospc.com

Abstract. Cryogenics and superconductivity (SC) have profoundly advanced biomedical technologies, particularly in areas such as cryosurgery, SQUID-based diagnostics, MRI and NMR imaging, and SC radiation therapy. These technologies have enabled the development of precise, minimally invasive medical procedures and highly sensitive diagnostic tools. This paper reviews key technical achievements and explores emerging directions in the field. Notable developments include cryosurgical and cryoablation systems for treating cardiac arrhythmias and pulmonary conditions; superconducting gantries with full 360° rotation for precision proton and ion beam therapy; and superconducting quantum interference devices (SQUIDs), which remain the most sensitive instruments for detecting magnetic fields, enabling advanced neurological and organ-level diagnostics. The paper also examines high-field MRI systems (ranging from 1.5 T to 11 T) for whole body and critical organs, ultra-high-field NMR spectroscopy (up to 21 T) for in-cell structural biology, the low magnetic field (mT) MRI using SQUID, and the cryogenic preservation. These innovations demonstrate the transformative impact of cryogenics and superconductivity on the future of biomedical science and healthcare.

1. Introduction

Cryogenics and superconductivity (SC) are transforming biomedical science through their integration into advanced diagnostic and therapeutic technologies. Their applications span cryosurgery, SQUID-based diagnostics, magnetic resonance imaging (MRI), nuclear magnetic resonance (NMR), and superconducting radiation therapy. This paper reviews significant achievements in these areas during the 50 years of innovations and highlights emerging directions. Notable developments include cryosurgical, or cryoablation, systems used to destroy various cancer tumors, treat cardiac arrhythmias, treat abnormal uterine bleeding, etc., and superconducting gantries capable of full 360° rotation that enable precise proton and ion beam therapy. Superconducting quantum interference devices (SQUIDs), the most sensitive magnetic field detectors to date, support high-resolution neurological and organ-level diagnostics etc. Advancements in imaging include high-field MRI systems operating between 1.5 T and 11 T for whole-body and critical organ scans, ultra-high-field NMR spectroscopy reaching up to 21 T for in-cell structural biology, and low-field (mT) MRI techniques using SQUIDs. Cryogenic preservation is also discussed. These developments illustrate how cryogenics and superconductivity are reshaping modern healthcare and paving the way for future innovations in biomedical technology in the world.

Content from this work may be used under the terms of the Creative Commons Attribution 4.0 licence. Any further distribution of this work must maintain attribution to the author(s) and the title of the work, journal citation and DOI.
Published under licence by IOP Publishing Ltd

2. Cryosurgery and Cryopreservation

Cryosurgery, or cryoablation, uses extremely low temperatures to freeze and destroy unwanted tissue, often cancerous. It is among the most important medical advances in the past 50 years [1], enabling minimally invasive treatment of internal organs. This success stems from advances in cryobiology, imaging (ultrasound or US, CT, MRI), small-diameter cryoprobe refrigeration (1–5 mm), and understanding of cryoablation's immunological effects. Access to internal organs is achieved percutaneously (skin puncture), via leg veins using catheters, or through natural openings (e.g., transbronchial lung ablation). The modern era of cryosurgery began in 1961 with Cooper and Lee [2], who used coaxial, vacuum-insulated cryoprobes with liquid nitrogen (LN_2) to target deep tissue. These developments laid the foundation for today's image-guided procedures. Rubinsky's review [1] highlights the critical role of imaging in guiding cryoprobe placement and monitoring ice ball formation. Together, these innovations have made cryoablation a safe and effective alternative to more invasive surgical approaches.

2.1 *Mechanisms of Cell Destruction*

Effective and safe cryosurgery requires an understanding of the mechanisms of cell destruction, which

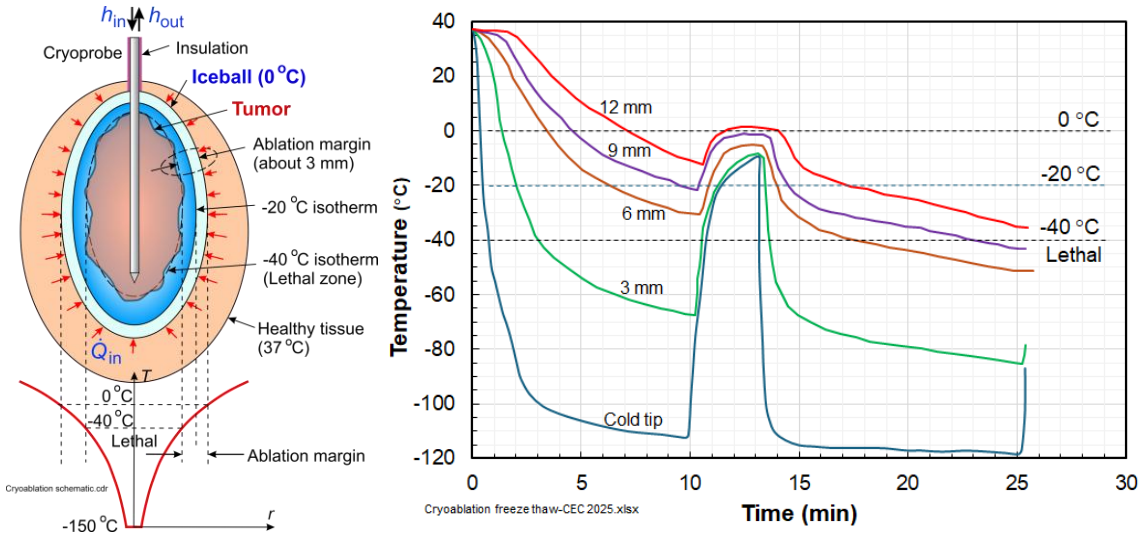

Figure 1. Left: Schematic of cryoablation isotherms showing tumor, ice ball, and ablation margins. Right: Example of freeze/thaw ablation in the first cycle [4].

is influenced by [4]: (a) *cooling rate:* Faster is more destructive. (b) *Tissue temperature:* Temperatures below -40 °C are lethal even for cancer cells, whereas temperature below -20 °C may cause death to some beneficial tissue. Margins of 3-5 mm are typical as shown in Fig. 1-Left. (c) *Time at lowest temperature*: Prolonged times in the transition region between -40 and -20 °C cause more cell destruction. (d) *Thawing rate*: Slow thawing is more lethal. (e) *Repetition*: Repetition leads to more cell destruction. Figure 1-Right is a typical freeze thaw process during the first cycle [3].

2.2 *Cryosurgical Technology, Systems and Cryosurgical Examples*

Commercial portable cryoablation consoles usually come equipped with ultrasound imaging equipment that allows the surgeon to insert the cryoprobe cold surface within the tumor and monitor the ice ball formation. Liquid nitrogen (LN_2) and Joule-Thomson (JT) are two main types of cryoablation systems in use today.

LN_2 systems: LN_2 systems use liquid nitrogen in various forms for cryoablation. Dermatologists employ hand-held dewars with spray tips for surface lesions. For internal tissue, LN_2 circulates through vacuum-insulated lines from a supply dewar to the cryoprobe and back. However, saturated LN_2 in long conduits

causes flow oscillations and the Leidenfrost effect. Modern systems solve this by compressing the liquid above its 34 bar critical pressure using pumps. Baust [5] describes a system operating at 60–90 bar, achieving fast cooling with flow rates of 3–4 g/s and refrigeration powers up to 325 W. These systems reach cryoprobe temperatures as low as -150 °C, Fig 2-Left. Cryosurgical devices have advanced through efforts by research institutions and industry. Fig 2-Right shows a multifunctional instrument with an 8-liter LN_2 dewar, pressure control, vacuum-insulated line, thermocouple needles, and interchangeable cryoprobe tips with optional heating and heat-exchange [6]. Tip enhancements include copper fins or powders for improved freezing during medical treatment.

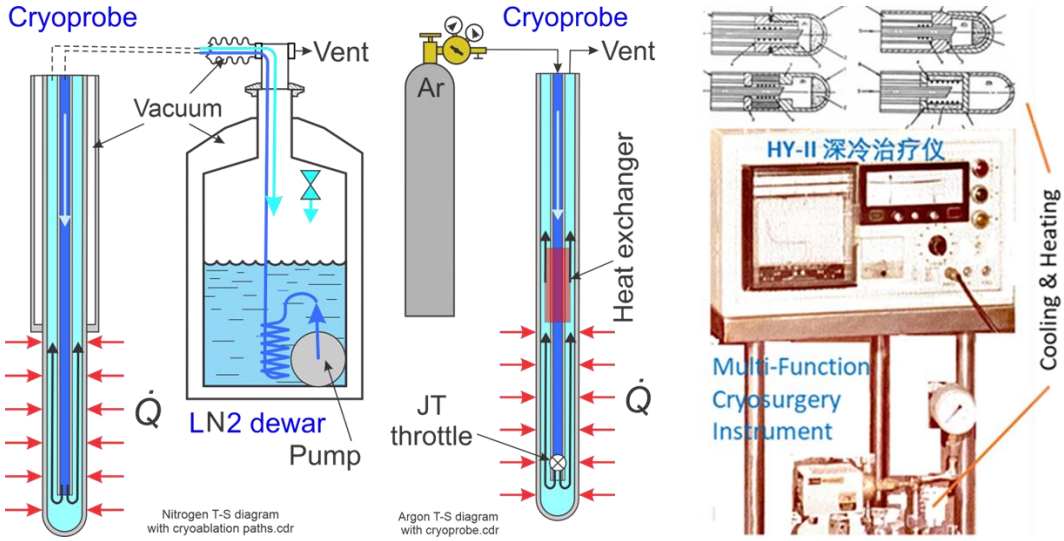

Figure 2. Left, Structure of a liquid nitrogen cryoprobe (Not to scale). Center, Structure of a JT cryoprobe (Not to scale). Right, Photo of a multifunction cryosurgery instrument with optional tips [6].

JT systems: JT systems use isenthalpic expansion of high-pressure gases to provide cooling. Argon (Ar) and nitrous oxide (N_2O) cryoablation systems have been developed in the last 30 years. Argon systems use a pressure of about 200-300 bar and can achieve liquefaction at -186 °C while N_2O systems use a pressure of 54 bar and achieve a temperature of -90 °C. With JT cooling the incoming gas is at ambient temperature, which alleviates the need for vacuum insulation along the lines, but the high-pressure gases must be supplied by bulky gas cylinders. Also, a heat exchanger is required to reach liquefaction temperatures, as shown in Fig 2-Center. The heat exchanger can be in the cryoprobe handle, but some miniature tip heat exchangers have been investigated [7-8]. Research on mixed refrigerant JT systems for cryoablation began in the 1990s and led to some commercial products that use refrigeration compressors for a closed-loop system [8].

Cryosurgical examples: Cryoablation is approved for treating tumors in the lungs, prostate, liver, kidney, bone, and breast, as well as for atrial fibrillation and endometrial ablation in women with abnormal uterine bleeding. Atrial fibrillation treatment involves inserting a 1-meter long and 3-millimeter diameter catheter through a leg vein to access the heart. The target is the pulmonary vein's junction with the heart. An innovative technique uses a balloon near the catheter tip to block blood flow and freeze the entire circumference. Liquid nitrogen or nitrous oxide is sprayed inside the balloon, freezing the contact area and simplifying the procedure in this challenging environment. The procedure is now commonly used to treat atrial fibrillation, which occurs in about 5 % of the US adult population.

2.3 *Cryopreservation*

The goal in cryopreservation is to prevent lethal intercellular ice formation during cooling. Two major factors that reduce the chance are slow cooling and the use of cryoprotectants. Cooling rates of 0.3-1

°C/min are typical. The other successful approach, known as vitrification, is to provide extremely high cooling rates around 10,000 ºC/min, which can only be achieved in small sample volumes of a few µL or less. Storage temperatures below -130 °C (143 K) are required to maintain long-term viability and to completely stop biological activity. Cryopreservation has numerous applications in medicine, fertility, research, agriculture, and beyond.

3. MRI and NMR for Biomedical

3.1 *Magnetic Resonance Imaging (MRI)*

MRI is based on nuclear magnetic resonance (NMR) where the energy levels of an atomic nucleus of non-zero nuclear spin are split in a magnet field. Transmitted radio waves with this same energy (resonance frequency) are absorbed by the nucleus and re-radiated as they relax. The energy splitting depends on the chemical environment of the nucleus and is proportional to the magnetic field. MRI uses this information to construct images of the distribution of hydrogen nuclei (protons) in the human body. The signals from cancerous tissue differ from those of healthy tissue.

Advances in superconducting NbTi, in the mid-1960s led to the first commercial application of superconducting magnets for MRI in the 1980s [9-11]. A field strength of 1.5 T has become the industry standard, but some 3 T, 7 T, and 11.7 T systems are in use for improved resolution.

MRI has now become the largest commercial application of superconductivity with over 35,000 superconducting MRI systems in operation worldwide. Approximately 3000 systems per year are sold.

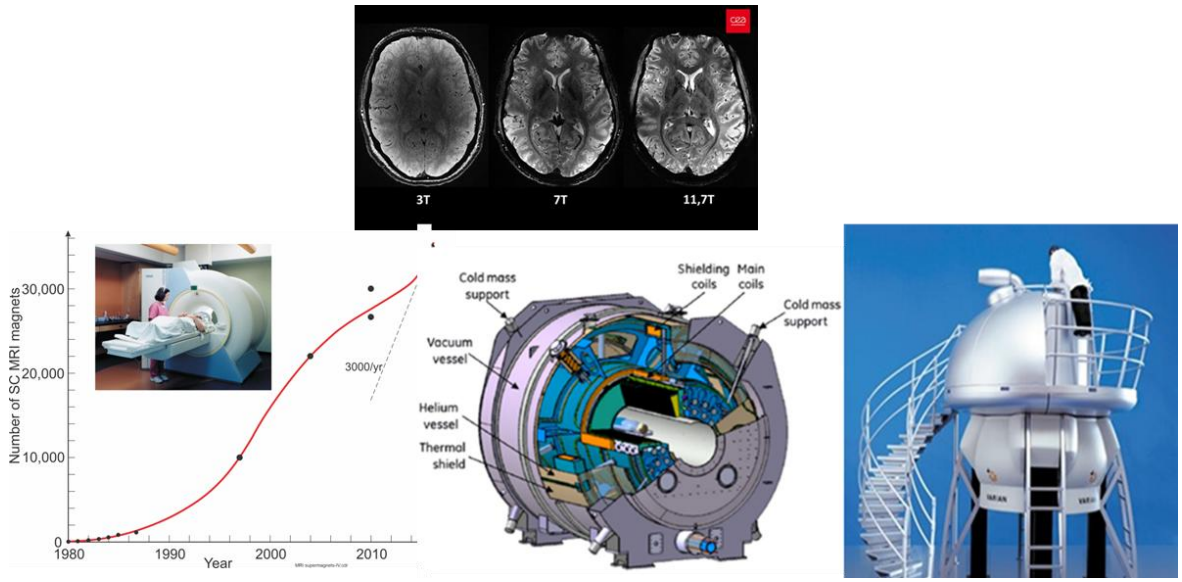

Figure 3. Left, Superconducting MRI systems in use around the world. Inset: Modern MRI system with a 1.5 T SC magnet and cryocooler, photo: Siemens. Center, 11.7 T Whole Body MRI [11]. Right, 900 MHz (21.1 T) NMR system, Photo: Varian. Upper, MRI images with deferent magnetic field, the higher fields the higher resolutions.

Figure 3 shows a typical 64 MHz 1.5 T MRI and the growth of superconducting MRI over time [9-11]. By the mid-1990s 4 K GM cryocoolers became commercially available, which led to zero boil-off magnets. These MRI systems still use about 1500 L of liquid helium for good heat transfer. In 2018 the first helium-free MRI systems were developed and deployed. The helium is sealed within the magnet space during manufacture and liquefied by the cryocooler. They use 7 L of LHe but require no vent. Nicolas Boulant reported the 11.7 T whole body MRI system (photo in Fig 3-Center). There is an interesting development to use of SQUID sensors to detect kHz rather than MHz frequencies, allowing operation at milli-tesla fields rather than tesla-level fields. This has the potential to significantly reduce installation and operating costs [12].

3.2 *NMR for Analyzing Biomacromolecules*

Nuclear Magnetic Resonance (NMR), widely used in MRI imaging, is also a key tool for analyzing biomacromolecules. Over the past 50 years, it has become essential for determining protein structures, typically requiring 2–50 mg of sample. High magnetic fields are necessary to study large macromolecules; for example, 21 T fields enable 900 MHz resonance, allowing analysis of proteins up to 30,000 molecular weights. In 2020, a 1.2 GHz system using 28.2 T magnets made of YBCO, Nb_3Sn, and NbTi was introduced, featuring a 54 mm room-temperature bore. NMR is helping uncover disease mechanisms in cancer, Alzheimer's, Parkinson's, cardiovascular conditions, and viral infections.

4. Superconducting Quantum Interference Devices (SQUID) for Medical Diagnostics

Electrical measurements of physiological potentials are well established in diagnostics, with magnetic counterparts like magnetocardiograms (MCG) and magnetoencephalograms (MEG). Biomagnetic research covers major organs, detecting signals from DC to hundreds of Hertz and fields from 50 fT to 10^5 fT (e.g. cardiogram ~ $5x10^4$, myogram ~ $4x10^3$, peripheral nerve ~ 10^3, evoked cortical activity ~ 60 fT, etc.) [13,14]. Some magnetic measurements, such as detecting ingested ferromagnetic materials, lack electrical analogs. SQUIDs offer the highest sensitivity: LTS SQUID ~ 1 fT and HTS SQUID ~ 20 fT. Biomagnetic SQUIDs systems must be magnetically transparent, using low-susceptibility materials like G-10 for dewars, which have typical coil-to-room T distances of ~2.5 cm and curved tails (Fig. 4).

4.1 *Biomedical Applications of SQUID Instruments*

Physiological magnetic fields vary in intensity, frequency, and distribution, requiring specialized, non-invasive measurement techniques. Whole-head MEG systems use hundreds of sensors, with dewars having 15–20 mm gaps. Coil-in-vacuum designs reduce gaps to ~5 mm, minimizing helium loss and vibration. MCG systems measure the vertical (B_z) field, using second-order gradiometers to improve fetal MCG [15-17]. Multi-channel systems (7–19 channels) measuring all three field components are used in gastroenterology, magnetoenterography, magnetomyography, and magnetoneurography. SQUID biomagnetometers measure liver iron concentration (Fig 5-Left). Magnetopneumography (MPG) monitors lung magnetizable materials, detecting fields as low as 1 nT [17].

4.2 *Dewar Design for SQUID in Biomedical Application*

For measuring external magnetic fields (e.g., NDE or biomagnetism), minimizing the distance between detection coils and room temperature is crucial [18-19]. This distance, or "tail gap," depends on the dewar tail diameter (Fig 4). The inner and outer tailpieces must be thick enough to withstand atmospheric pressure differences without deforming. For instance, a 25-cm-diamter disk experiences a force of ~5 N (½ ton) under a 1-atmosphere differential. Tailpiece thickness is determined by acceptable deflection, typically limited to ≤0.1 mm. Larger dewars require thicker plates to control deflection.

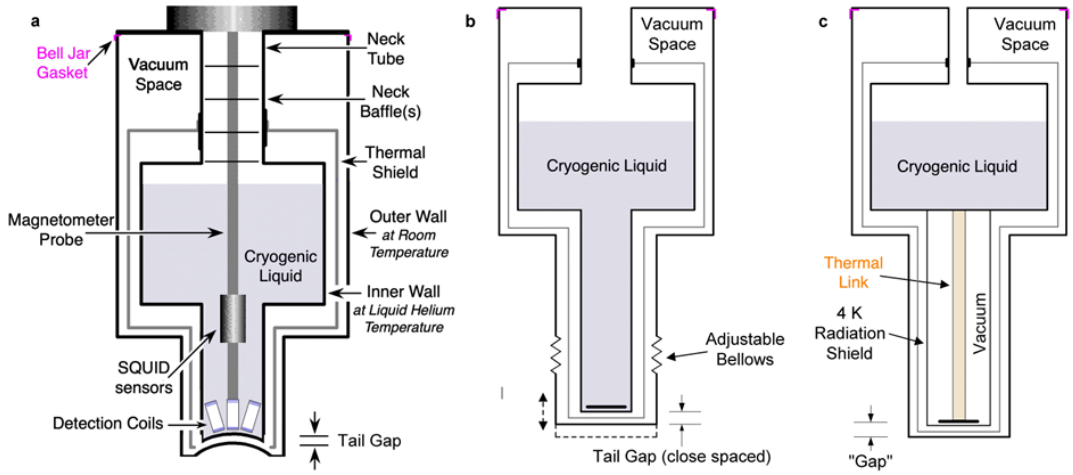

Figure 4. Different methods of achieving close dewar tail spacing. MLI is omitted for clarity.

As dewar materials contract when cooled, the tail gap increases. G-10 contracts ~0.3% from 300 K to 4.2 K, meaning a 1-meter dewar with nearly touching tails at room temperature would have a 3 mm gap at helium temperature. Various mechanisms can counteract this effect.

Adjustable Tail Mechanisms. A bellows or similar vacuum-tight component in the outer tail (Fig 4-Center) can reduce coil-to-sample spacing and compensate for thermal contraction.

Coil-in-Vacuum. This approach replaces liquid immersion by thermally linking detection coils to the cryogen bath, eliminating the need for an inner tail and reducing coil-to-sample distance (Fig. 4-Right). High thermal conductivity materials (e.g., copper, sapphire) serve as thermal links, maintaining SQUID sensors below their Tc (e.g., 9.3 K for NbTi). This reduces MLI requirements and allows even closer spacing.

Coil-in-vacuum cryostats also benefit from adjustable tail mechanisms. Since probes are not inserted down a neck tube, these dewars can have narrower necks, lowering heat load and extending hold times. Another method mounts detection coils on low thermal conductivity standoffs fixed to the dewar tail, enabling sub-mm coils to be positioned within 200 μm of room temperature while remaining near liquid helium temperatures.

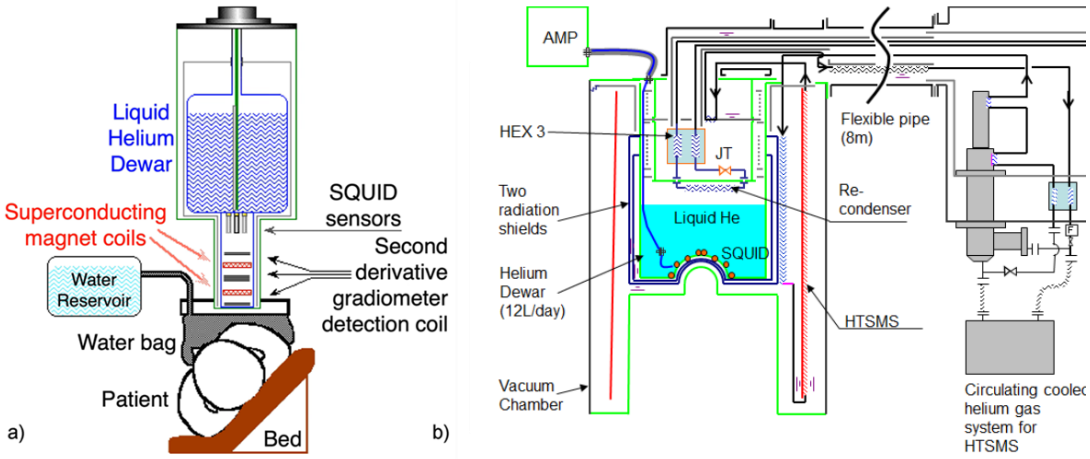

Figure 5 Left, coil-in-vacuum system for combining SQUID sensors and superconducting magnetic to measure magnetic susceptibility of internal organs [16]. Right, diagram of a MEG system utilizing a remote liquefier/recondenser to achieve zero boiloff [20].

For applications with significant magnetic fields near the detection coil, helium bubbles can induce low-frequency noise due to the magnetic susceptibility difference between liquid and gas phases. Coil-in-vacuum technology (Fig 5-Left) has been used to measure the magnetic susceptibility of the liver and quantitatively determine hepatic iron stores. The use of reliquefiers (Fig 5-Right) has allowed MEG systems to be used in clinical systems with zero boil-off significantly reducing operating costs [20].

5. Superconducting Compact Accelerator and Gantry in Proton and Ion Therapy

5.1 *World First Superconducting Rotating Gantry for Ion-Therapy*

In general, a SC rotating gantry offers three key advantages: 1) No need to rotate the patient, 2) Precise multi-directional dose distribution, and 3) Intensity Modulated Particle Therapy (IMPT) as shown in Fig 6 left [21-24]. In 2015, Iwata reported the world's first superconducting (SC) rotating gantry at NIRS/HIMAC (Fig 7 Right) [25]. Designed for ^{12}C ions with 3D scanning, it employs six 2.88 T combined-function SC magnets, reducing its mass to under 300 metric tons and length to 13 m, with a 5.45 m beam orbit radius. It delivers 430 MeV beams with a 30 cm range in water in technical tests.

5.2 *Various Advanced Design of SC Gantries and Synchrotrons*

Among various design and development from many institutes, Benedetto et al reported the conceptual design of a new compact SC gantry and synchrotron for carbon ion therapy and focuses on the solutions (layout and optics) to make it compact [24]. The main feature of this gantry design is that it is smaller and lighter compared to existing carbon-ion gantries. This is achieved by adopting an innovative mechanical design and by using SC magnets of the canted cosine theta type with a small aperture. The optics are optimized to reduce the beam size; they are achromatic and independent of the rotation angle (for an incoming round beam), as shown in Fig. 6. A preliminary synchrotron layout based on similar SC magnets units is presented and the dose delivery specificities are discussed [24].

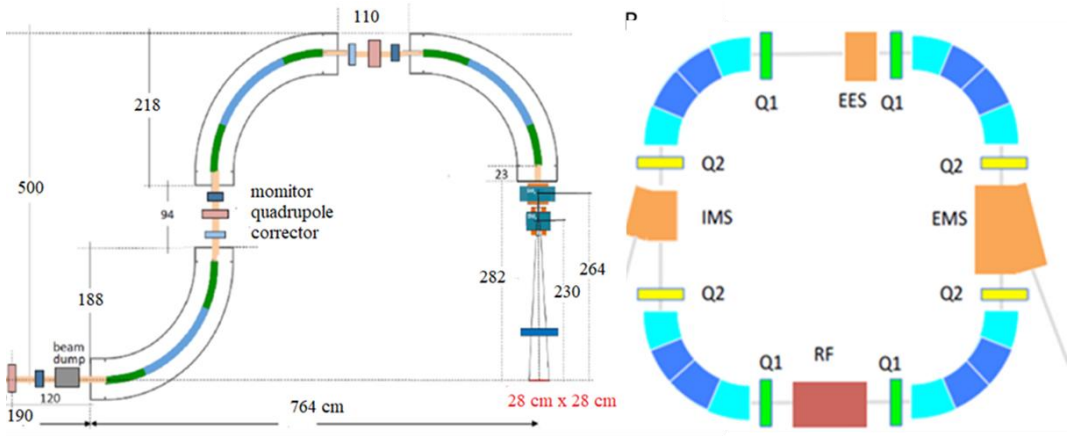

Figure 6. Right, Lay out of the synchrotron. Left, Layout of the 4-T gantry, the quadrupole coils inside the main CCT magnets. [24]

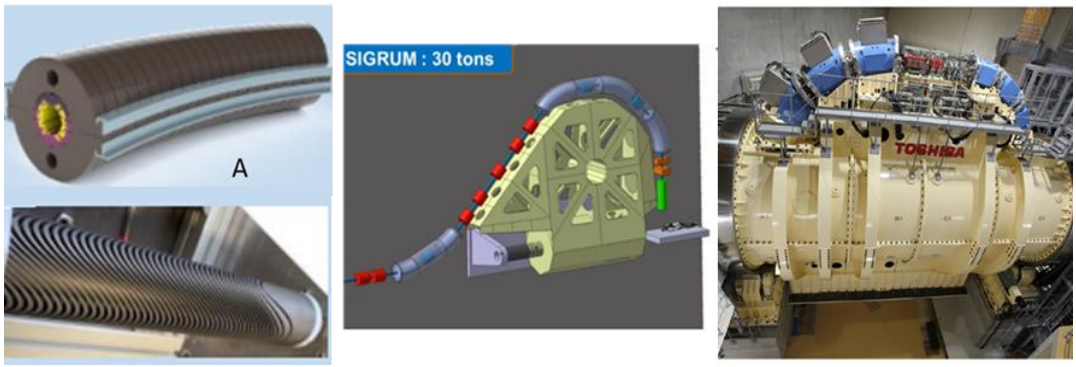

Figure 7. Right, SC gantry capable of 360^0 rotations at NIRS/HIMAC [25]. Left, Curved SC magnets combining dipole & quadrupole, and Center, SC rotating gantry designed for NIMMS [26].

5.3 *Research and Development of Next Ion Medical Machine Study (NIMMS) at CERN*

The Next Ion Medical Machine Study (NIMMS), launched at CERN in 2018 with support from CERN's KT for Medical Applications, aims to develop technologies for next-generation ion cancer therapy accelerators [26]. NIMMS focuses on four areas: (1) compact superconducting (SC) synchrotrons for enhanced performance; (2) curved SC magnets using canted cosine theta (CCT) designs with NbTi or HTS materials (Fig. 7-Left); (3) SC gantries for precise, multi-angle beam delivery (Fig. 7-Center); and (4) high-frequency ion linacs with compact, bent layouts. SC magnets integrate dipole and quadrupole functions in CCT windings. Two main designs are proposed: dipoles with peak field (Bp) 6.6 T, ramp rate 1 T/s, and radius 2.2 m; and quadrupoles with gradients of 4.0 T/m and Bp up to 7 T. Development

requires global collaboration, such as the European consortiums HITRI-plus and IFAST, to address technical challenges and meet the precision demands of medical accelerator systems.

Acknowledgements
The authors express our sincere gratitude to our colleagues and the conference publishers for granting us permission to cite/use their published figures in the review paper.

References

[1] Rubinsky, B., 2000 *Cryosurgery*, Annu. Rev. Biomed. Eng. 157-187 2000.
[2] Cooper I. and Lee, A, "Cryostatic congelation; a system for producing a limited controlled region of cooling or freezing of biological tissues," *J. Nerv. Ment. Dis*. 133, 259-263 (1961).
[3] Gage, A. and Baust, J., Mechanisms of tissue injury in cryosurgery, *Cryobiology* 37, 171-186 (1998).
[4] Dobak, J, A review of cryobiology and cryosurgery, *Advances in Cryogenic Engineering*, 43, 1998. 889-896
[5] Baust J.M, Robilitt A, Gage A, Baust J.G, 2016 Enhanced Cryoablative Methologies, Chapter 1 in Multiscale Technologies for Cryomedicine, World Scientific Publishing, 2016.
[6] Shu Q-S, Xie A-F, Hu S-S, Tao X-L, Lu S-T, 1981 Cryo-neurosurgery machine system, process technology and theory, Conference by International Institute of Refrigeration, Commission C1, June Warszawa, Poland 1981.
[7] Marquardt, E, Radebaugh R, and Dobak J, A cryogenic catheter for treating heart arrhythmia, *Advances in Cryogenic Engineering*, 43, 903-910 (1998).
[8] Boiarsk, M et al, Retrospective of mixed refrigerant technology and modern status of cryocooler based on one-stage, oil-lubricated compressors. *Advances in Cryogenic Engineering, 43*, 1701-1708
[9] Schwall RE. 1987. MRI--Superconductivity in the marketplace. *IEEE Trans. on Superconductivity MAG-23*: 1287-93, 1987.
[10] Radebaugh R. and Bar-Cohen Y, Low temperature materials and mechanisms-Applications and challenges, Chapter 14 in: *Low Temperature Materials and Mechanisms*, CRC Press 2016.
[11] Boulant, N., Mauconduit, F., Gras, V. et al. In vivo imaging of the human brain with the Iseult 11.7-T MRI scanner. *Nat Methods* 21, 2013–2016 (2024). https://doi.org/10.1038/s41592-024-02472-7
[12] Sarracanie, M and Salameh, N., 2020 Low-Field MRI: How Low Can We Go? A Fresh View on an Old Debate, *Front. Phys*., 8, 172 (2020); doi: 10.3389/fphy.2020.00172
[13] Roth, B.J., Biomagnetism: The First Sixty Year, Sensors, 23, 4218 (2023); doi: 10.3390/s23094218
[14] Robinson, S. and Fagaly, R.L., Biomagnetic Instrumentation: Current Capabilities & Future Trends, *Proc. ASME*, AES-9, 7-12 (1989)
[15] Fagaly R.L, Superconducting quantum interference device instruments and applications, *The Review of Scientific Instruments,* 77, 101101 (2006)
[16] Brittenham, G.M., Farrell, D.E., Harris, J.W., Feldman, E.S.,et al., Magnetic-Susceptibility of Human Iron Stores, *New Eng. J. Med*., 307, 1671-1675 (1982)
[17] Stahlhofen W. and Möller W, Behaviour of magnetic micro-particles in the human lung, Radiat. Environ. *Biophys*., 32, 221-238 (1993).
[18] Warburton R.J., Reineman, R.C., Brinton, E. and R.L. Fagaly, R.L., Liquid Helium Ballast Refrigeration, *ColdFacts*, 39, 10 – 13 (2023)
[19] Sarwinski, R.E., Reineman, R.C., Gott, S,et al, Self-adjusting assembly and method for close tolerance Spacing, *United States Patent* No. 6,784,663 B2, (2004)
[20] Narasaki K et al., 2020 Development of zero boil-off cooling systems for superconducting self-shielded MEG, 2020 IOP Conf. Ser.: Mater. Sci. Eng. 755 012107
[21] Norman H, Steinberg A et al, 2021 Review of Technologies for Ion Therapy Accelerators, *12th Int. Particle Acc. Conf.* JACoW Publishing, 2021
[22] Edward W. Collings et al, 2022 Accelerators, Gantries, Magnets, and Imaging Systems for Particle Beam Therapy, www.frontiersin.org, February 2022 Volume 11 Article 737837 L
[23] Nesteruk K, et al, 2019 Large energy acceptance gantry for proton therapy utilizing superconducting technology, *Phys. Med. Biol*. arXiv:1901.01821v1, physics.med-ph, 7 Jan 2019L
[24] Benedetto E, Harbi N et al, 2022 A Carbon-Ion Superconducting Gantry and A Synchrotron Based on Canted Cosine Theta Magnets. *Physics in Medicine and Biology*, DOI: 10.48550/arXiv.2105.04205L
[25] Iwata Y, et al. 2018 Superconducting Gantry for Carbon-Ion Radiotherapy, *9th IPAC* 2018, Canada. Publishing. doi: 10.18429/JACoW-IPAC2018-TUZGBF
[26] Vretenar, Maurizio et al, 2021 The next ion medical machine study at CERN: Towards a next generation cancer research and therapy facility with ion beams*, IPAC 2021*, 10.18429/JACoW-IPAC2021-MOPAB413